Journal Pre-proof

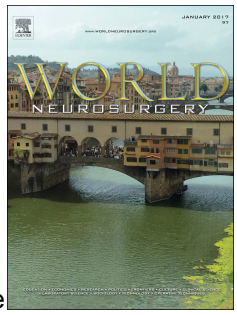

Intraoperative 3-T magnetic resonance spectroscopy for detection of proliferative remnants of glioma

Yuichi Fujita, MD, Masaaki Kohta, MD, PhD, Takashi Sasayama, MD, PhD, Kazuhiro Tanaka, MD, PhD, Mitsuru Hashiguchi, MD, Hiroaki Nagashima, MD, PhD, Katsusuke Kyotani, Tomoaki Nakai, MD, PhD, Tomoo Ito, MD, PhD, Eiji Kohmura, MD, PhD

PII: S1878-8750(20)30235-7

DOI: https://doi.org/10.1016/j.wneu.2020.01.217

Reference: WNEU 14247

To appear in: *World Neurosurgery*

Received Date: 27 October 2019

Revised Date: 28 January 2020

Accepted Date: 28 January 2020

Please cite this article as: Fujita Y, Kohta M, Sasayama T, Tanaka K, Hashiguchi M, Nagashima H, Kyotani K, Nakai T, Ito T, Kohmura E, Intraoperative 3-T magnetic resonance spectroscopy for detection of proliferative remnants of glioma, *World Neurosurgery* (2020), doi: https://doi.org/10.1016/j.wneu.2020.01.217.

Intraoperative 3-T magnetic resonance spectroscopy for detection of proliferative remnants of glioma

Yuichi Fujita, MD[1]; Masaaki Kohta, MD, PhD[1,*]; Takashi Sasayama, MD, PhD[1]; Kazuhiro Tanaka, MD, PhD[1]; Mitsuru Hashiguchi, MD[1]; Hiroaki Nagashima, MD, PhD[2]; Katsusuke Kyotani[3]; Tomoaki Nakai, MD, PhD[1]; Tomoo Ito, MD, PhD[4]; Eiji Kohmura, MD, PhD[1]

[1]Department of Neurosurgery, Kobe University Graduate School of Medicine, Kobe, Hyogo, Japan

[2]Department of Neurosurgery, Massachusetts General Hospital Research Institute, Boston, MA, USA

[3]Center for Radiology and Radiation Oncology, Kobe University Graduate School of Medicine and Kobe University Hospital, Kobe, Hyogo, Japan

[4]Department of Diagnostic Pathology, Kobe University Graduate School of Medicine, Kobe, Hyogo, Japan

*Corresponding author: Masaaki Kohta

Department of Neurosurgery, Kobe University Graduate School of Medicine, 7-5-1 Kusunoki-cho, Chuo-ku, Kobe, Hyogo 650-0017, Japan

Phone: +81-78-382-5966; Fax: +81-78-382-5979

E-mail: kohta@med.kobe-u.ac.jp

Key words: Intraoperative magnetic resonance imaging; Magnetic resonance spectroscopy; Glioma; Choline; N-acetyl-L-aspartate; Cho/NAA

Short title: Intraoperative MRS for glioma

Intraoperative 3-T magnetic resonance spectroscopy for detection of proliferative remnants of glioma

Abstract

Objective: Few studies have examined the usefulness of intraoperative magnetic resonance spectroscopy (iMRS) for identifying abnormal signals at the resection margin during glioma surgery. The aim of this study was to assess the value of iMRS for detecting proliferative remnants of glioma at the resection margin.

Methods: Fifteen patients with newly diagnosed glioma underwent single-voxel 3-T iMRS concurrently with intraoperative MRI-assisted surgery. Volumes of interest (VOIs) were placed at T2-hyperintense or contrast-enhancing lesions at the resection margin. In addition to technical verification, the correlation between the MIB-1 labeling index (a pathological feature) and metabolites measured by using iMRS (N-acetyl-L-aspartate [NAA], choline [Cho], and the Cho/NAA ratio) was analyzed.

Results: iMRS was performed for 20 VOIs in 15 patients. Fourteen (70%) of these VOIs were confirmed to be MIB-1-positive. There was a significant positive correlation between Cho/NAA ratio and MIB-1 index ($r = 0.46$, $p = 0.04$). Cho level ($p = 0.003$) and Cho/NAA ratio ($p = 0.002$) were significantly higher in VOIs that were MIB-1-positive than in those that were MIB-1-negative. Detection of a Cho level >1.074 mM and a Cho/NAA ratio >0.48 using iMRS resulted in high diagnostic accuracy for MIB-1-positive remnants (Cho level, sensitivity 86%, specificity 100%; Cho/NAA ratio, sensitivity 79%, specificity 100%).

Conclusions: This study provides evidence that 3-T iMRS can detect proliferative remnants of glioma at the resection margin using Cho level and Cho/NAA ratio, suggesting that intraoperative MRI-assisted surgery with iMRS would be practicable in glioma.

INTRODUCTION

Surgery plays a crucial role in the treatment of glioma. The most extensive resection possible with preservation of neurological function is the most desirable strategy because the removal rate affects prognosis.[1–4] Intraoperative magnetic resonance imaging (MRI) is a useful tool in this regard because it can detect tumor remnants and identify unexpected complications during surgery.[5–7] Intraoperative MRI allows neurosurgeons to operate with updated neuronavigation, which corrects for the brain shift phenomenon that occurs because of the effects of gravity, loss of cerebrospinal fluid, and deformation in response to resection.[6,8,9] Intraoperative 3-T MRI has been used for glioma surgery at our institution since March 2015. However, despite the clear advantages of intraoperative MRI, it is difficult to determine whether T2-hyperintense or contrast-enhancing lesions seen at the resection margin using this method represent residual tumor or a non-tumoral change. Accurate judgment of the resection margin is key to the success of intraoperative MRI-assisted glioma surgery.

Magnetic resonance spectroscopy (MRS) is non-invasive and provides important information on metabolic tissue components, such as N-acetyl-L-aspartate (NAA), choline (Cho), and creatine (Cr). NAA is a neural marker and Cho is involved in membrane turnover. Increased Cho, Cho/Cr, and Cho/NAA and decreased NAA generally suggest malignancy.[10–13] Using this information for brain tumors, preoperative MRS could assist in detection and grading of glioma.[10,14] MRS also provides molecular information, such as isocitrate dehydrogenase (IDH) mutation status, which is a key genetic aberration that can be used for differentiation of glioma.[15] We have previously reported that preoperative detection of glutamate and 2-hydroxyglutarate by 3-T MRS results in high diagnostic accuracy (sensitivity 72%, specificity 96%) for IDH-mutant glioma.[16] Preoperative MRS is becoming an essential diagnostic modality in determining the treatment strategy for glioma. However, few studies have examined the value of intraoperative MRS (iMRS) in glioma surgery.[17,18] Considering

the clinical impact of preoperative MRS, intraoperative use of MRS can be expected to be useful for differentiating abnormal signals seen on intraoperative MRI. Therefore, we hypothesized that iMRS could detect proliferative remnants at the resection margin by detecting major metabolites, namely, Cho and NAA. The aim of this study was to test this hypothesis and to investigate the technical aspects of applying conventional preoperative MRS to iMRS for glioma surgery.

MATERIAL AND METHODS

Study design

The study was approved by the institutional review board at our institution (protocol number 160185) and conducted according to the institutional and national ethical guidelines and in accordance with the Helsinki Declaration. Written informed consent was obtained from all patients prior to enrollment in the study. Fifteen patients with newly diagnosed glioma who underwent intraoperative MRI-assisted surgery with iMRS at our institution were included in the study.

Our intraoperative 3-T MRI facility is designed based on a twin-room concept as described previously.[5] The patient's head is fixed with disposable cranial pins in a 3-T MRI-compatible headrest-head coil unit. Surgery is performed in the usual manner using a neuronavigation system with electrophysiological monitoring. Patients with a tumor close to Broca's area underwent awake surgery. At the step when it was assumed that a planned region could be removed, we performed intraoperative MRI and checked for abnormal signals suggesting residual tumor tissue. The intraoperative MRI protocol included diffusion-weighted imaging (DWI; b-values, 0 and 1000 s/mm^2; repetition time (TR)/echo time (TE) 5600/63 ms; field of view [FOV], 260 mm × 260 mm; matrix, 154 × 180; slice thickness, 4 mm; slice gap, 1 mm; flip angle, 90°); T2-weighted imaging (T2WI; TR/TE, 4070/108 ms; FOV, 227 mm × 260

mm; matrix, 358 × 448; slice thickness, 5 mm); T2-weighted fluid-attenuated inversion recovery (TR/TE, 11,000/120 ms; FOV, 227 mm × 260 mm; matrix, 256 × 256; slice thickness, 5.0 mm); three-dimensional T1-weighted imaging (T1WI; TR/TE, 2300/2.3 ms; FOV, 320 mm × 320 mm; matrix, 320 × 320; slice thickness, 1.0 mm) before and after injection of intravenous gadolinium contrast agent (0.2 ml/kg, Magnescope, Guerbet, Paris, France).

iMRS was performed concurrently in this study. Volumes of interest (VOIs) were placed at the resection margin where either T2WI or contrast-enhanced T1WI (CE-T1WI) was suggestive of residual tumor. The intraoperative MRI data were then re-registered for the patient using iPlan Cranial (BrainLAB AG, Feldkirchen, Germany), and the site corresponding to the VOI on iMRS was selectively biopsied using the updated neuronavigation system for histological evaluation before additional resection. The proliferation potential in the resection margin was evaluated using the MIB-1 index; the correlation between this pathological parameter and metabolites measured by iMRS (Cho and NAA levels and the Cho/NAA ratio) was analyzed. Finally, the accuracy of iMRS for detection of proliferative remnants was examined. The details of the iMRS procedure and histopathological analysis are described in the following subsections.

The extent of resection was evaluated on MRI scans obtained within 72 h of surgery. Almost complete resection (>95%) of T2-hyperintense or contrast-enhancing lesions was considered to be gross total resection, incomplete resection (90%–95%) as subtotal resection, and further incomplete resection (50%–90%) as partial resection.

iMRS procedure and analysis of metabolites

The iMRS signal was acquired using a 3-T MRI/^{1}H-MRS scanner (Magnetom Skyra, Siemens Healthcare, Erlangen, Germany). A quadrature body coil was used for transmission

of the radiofrequency pulses and an eight-channel head coil for signal reception. Double-echo point-resolved spectroscopy (PRESS) with chemical-shift selective water suppression was used to acquire single-voxel localized MR spectra. Single-voxel iMRS acquisition parameters were as follows: VOI, 1.5 × 1.5 × 1.5 cm^3; TR/TE, 2000/35 ms; number of acquisitions, 128 averages; and 1024 complex points for the spectral data. A VOI was placed at the resection margin where hyperintense signals on T2WI or effects of contrast enhancement on CE-T1WI were shown on intraoperative MRI while avoiding contamination by cerebrospinal fluid or hematoma.

iMRS data were quantified using LCModel version 6.3 (Stephen Provencher, Montréal, QC, Canada). Absolute metabolite concentrations (mM) were estimated using an unsuppressed water signal as a reference. Metabolite measurements with Cramér-Rao lower bounds (CRLB) below 30% were used. Cho and NAA levels and the Cho/NAA ratio were examined.

Histopathological analysis

Histopathologic diagnosis was made according to the 2016 World Health Organization (WHO) guidelines.[19] The tissue corresponding to the VOI on iMRS was selectively biopsied using the updated neuronavigation system. MIB-1 was confirmed by immunohistochemistry using a specific antibody (clone MIB-1, monoclonal, 1:200; Dako, Carpinteria, CA). MIB-1 staining was scored by a neurosurgeon (MK or TS) and reviewed by a neuropathologist (TI) without knowledge of the clinical data. ImageJ 1.48 software (National Institutes of Health, Bethesda, MD) was used to analyze the images. The mean percentage of positively stained nuclei was calculated from five randomly selected fields per section under ×200 middle-power magnification. The final MIB-1 index was classified as positive (MIB-1 ≥1%) or negative (MIB-1 <1%) as described elsewhere.[20]

Statistical analysis

Pearson's correlation coefficient was used to assess the linearity of the relationship between the MIB-1 index and metabolites detected by iMRS. The Mann-Whitney *U* test was used for comparisons between two groups. The area under the receiver-operating characteristic (ROC) curve was used to investigate the diagnostic performance of iMRS. All statistical analyses were performed using EZR (Saitama Medical Center, Jichi Medical University, Saitama, Japan), which is a graphical user interface for R (R Foundation for Statistical Computing, Vienna, Austria).[21] A two-sided p-value of <0.05 was considered statistically significant.

RESULTS

Patient characteristics

The 15 patients consisted of 10 men (67%) and 5 women (33%) of median age 62 (range 33–85) years (Table 1). WHO grade II glioma (diffuse astrocytoma, oligodendroglioma) was histologically confirmed in 2 patients (13%), grade III glioma (anaplastic astrocytoma) in 3 (20%), and grade IV glioma (glioblastoma) in 10 (67%). Seven tumors (47%) were in the frontal lobe, 4 (27%) were in the temporal lobe, 2 (13%) were in the parietal lobe, and 2 (13%) were in the insula. Eleven tumors (73%) were in the right cerebral hemisphere and 4 (27%) were in the left. Two patients (cases 2 and 6) underwent awake surgery. Gross total resection was achieved in 11 patients (73%) and subtotal resection in the remaining patients (27%) because of involvement of the eloquent areas. Eleven (73%) of 15 patients showed recurrence (local in 5 [45%], distant in 6 [55%]) during a median follow-up period of 16 (range 9–53) months. All recurrences after subtotal resection were local and those after gross total resection (6 in 7 patients) were distant. There were no recurrences in the area corresponding to the VOIs in the patients with local recurrence.

Correlation between MIB-1 index and metabolites measured by iMRS

iMRS was performed for 20 VOIs in the 15 patients. The mean NAA level was 3.111 ± 2.010 mM (mean CRLB 16 ± 8%), the mean Cho level was 1.598 ± 0.978 mM (mean CRLB 10 ± 6%), and the mean Cho/NAA ratio was 0.64 ± 0.49. The mean MIB-1 index was 8.0 ± 8.7%. The Cho/NAA ratio had a significant positive correlation with MIB-1 index (r = 0.46 [95% confidence interval (CI) 0.02–0.75], p = 0.04). There was no significant correlation between MIB-1 index and NAA level (r = -0.18 [95% CI -0.58, 0.28], p = 0.44) or Cho level (r = 0.30 [95% CI -0.17, 0.65], p = 0.21; Fig. 1A). Of the 20 VOIs, 14 (70%) were confirmed to be MIB-1 positive. Cho level and Cho/NAA ratio were significantly higher in VOIs that were MIB-1-positive than in those that were MIB-1-negative (1.953 ± 0.944 mM vs. 0.771 ± 0.363 mM, p = 0.003 and 0.80 ± 0.50 vs. 0.30 ± 0.40, p = 0.002, respectively). There was no significant between-group difference in NAA level (3.103 ± 1.918 mM vs. 3.130 ± 2.209 mM, p = 0.72; Fig. 1B). Next, we used the ROC curve method to investigate whether the Cho level and Cho/NAA ratio on iMRS could be used to detect MIB-1 positivity. ROC curve analysis demonstrated that a Cho level >1.074 mM was 86% sensitive and 100% specific for MIB-1 positivity (area under the curve 0.91) and that a Cho/NAA ratio >0.48 was 79% sensitive and 100% specific for MIB-1 positivity (area under the curve, 0.92; Fig. 1C).

Illustrative cases

iMRS in case 4

A 40-year-old right-handed man presented with a brain tumor that had been detected incidentally during a routine medical checkup (Fig. 2). Preoperative MRI demonstrated a mass lesion with indistinct margins and no contrast enhancement in the right frontal lobe. After resection of the preoperatively scheduled lesion, intraoperative MRI showed residual T2-hyperintensity at the ventral and dorsal resection margins, where VOIs were set for iMRS.

The ventral VOI had a high Cho level of 2.571 mM (>1.074 mM). In contrast, there was no increase in either the Cho level (1.021 mM) or the Cho/NAA ratio (0.14) in the dorsal VOI. The MIB-1 index of the tissue corresponding to the ventral VOI was 1.4% (positive) and that corresponding to the dorsal VOI was 0.5% (negative). After intraoperative MRI with iMRS, complete resection was achieved by additional resection of the residual T2-hyperintense lesion. The integrated histological and molecular genetic diagnosis was WHO grade II oligodendroglioma, IDH1-mutant and 1p/19q-codeleted. There has been no postoperative neurological deterioration or recurrence as of 42 months after surgery. In this case, iMRS allowed accurate prediction of MIB-1 positivity and negativity. Additional resection for the ventral residual T2-hyperintensity was in retrospect the correct decision whereas additional resection for the dorsal T2-hyperintensity might have been excessive.

iMRS in case 7

A 35-year-old right-handed man presented complaining of episodes of convulsive seizures (Fig. 3). Preoperative MRI showed a mass lesion with indistinct margins and contrast enhancement in the right temporal lobe. After total resection of the contrast-enhancing lesion, intraoperative MRI showed residual hyperintensity on T2WI at the medial resection margin, where a VOI was set for iMRS. The VOI demonstrated a high Cho level of 3.451 mM (>1.074 mM) and a high Cho/NAA ratio of 2.06 (>0.48). The MIB-1 index of the tissue corresponding to the VOI was 13.6%. Finally, gross total resection was achieved by additional resection. The integrated histological and molecular genetic diagnosis was WHO grade IV glioblastoma, IDH1-mutant. This patient developed distant recurrence at 27 months postoperatively and died 6 months after the recurrence. The iMRS results in this patient accurately predicted MIB-1 positivity. In retrospect, the additional resection was considered to be the correct decision.

Discussion

We successfully performed 3-T iMRS based on our experience of preoperative MRS and intraoperative MRI and found that 3-T iMRS could detect proliferative remnants of glioma using Cho level and Cho/NAA ratio. A high-field MRI system (≥1.5 T) has technical advantages, including the ability to acquire high-resolution images, shorten the image acquisition time, and increase the chemical shift; its utility is further demonstrated on MRS. High-field intraoperative MRI is used in a number of centers. Even if the resection is performed with a navigation system based on preoperative MRI, unintentional tumor remnants might be shown on intraoperative images because of the gap in the navigation system caused by the brain shift phenomenon.[9] Intraoperative MRI allows additional resection of such residual tumors with the updated navigation system, leading to improvement of the tumor resection rate.[6,8] However, it is often challenging to determine whether the abnormal signals at the resection margin represent a residual tumor or non-tumoral change using intraoperative MRI. In contrast with studies that have led to advances in intraoperative use of MRI, there have been few studies on the usefulness of iMRS in surgery for glioma. Pamir et al.[17] were the first to report the value of iMRS for detecting residual tumor. However, they examined only low-grade gliomas (n = 14) using a long echo time (TE) (135 ms), a single voxel, a high-field (3 T), and VOIs that were 8 cm^3, larger than the typical size used in our study. Furthermore, they defined an increased Cho/Cr ratio, that is, 20% higher than that of an internal control, as residual tumor, resulting in high accuracy for identifying residual tumor (sensitivity 85.7%, specificity 100%). Roder et al.[18] examined both low-grade (n = 20) and high-grade (n = 25) gliomas using short-TE (30 ms) single-voxel 1.5-T iMRS. They measured NAA, Cho, and Cr using normal-appearing white matter as a reference. They found residual tumors in VOIs with increased Cho/NAA and

Cho/Cr ratios, although they did not confirm that VOIs with a low Cho/NAA or Cho/Cr ratio were non-tumoral changes pathologically. These are the only studies that have examined the usefulness of iMRS for glioma surgery, and there is still no clear iMRS methodology or criteria for detecting residual tumors.

The choice of whether to use single-voxel or multivoxel is particularly important in MRS methodology. Single-voxel spectroscopy is technically simple and can acquire data easily, and so is the most widely used method. However, it has the disadvantage of providing data from only a small portion of a lesion; hence, large and heterogeneous lesions such as glioblastoma not corresponding to the VOI might have different characteristics. On the other hand, multivoxel spectroscopy overcomes the shortcomings of single-voxel spectroscopy, but there are still some problems, such as longer set-up and imaging times, difficulties obtaining homogenous data over the entire region, and spectral contamination from adjacent voxels.[22–25] The technical difficulty of multivoxel spectroscopy increases further when used intraoperatively in that iMRS is targeting lesions at the resection margin that are smaller than the ones present preoperatively. There are other issues in MRS methodology, including whether to use short or long TE and PRESS or stimulated echo acquisition mode. While each has its own advantages and disadvantages, the optimal parameters for MRS in brain tumors are still controversial.[16,26,27] Furthermore, after a metabolite signal is acquired by MRS, post-processing to specify the peak and chemical shift of the waveform and to integrate the area under the peak is usually required to obtain a measurement value for each metabolite. Postprocessing may be associated with problems such as operator bias and difficulty in accurately separating overlapping signals. Previous reports on iMRS also had these problems and could not eliminate the reproducibility issue. LCModel software solves these problems[28] and was used in this study. This software can automatically perform quantitative analysis of typical metabolites just by reading the MRS data file and specifying the basis-set file

corresponding to the MRS conditions. Within this context, we decided to perform iMRS based on the following criteria with an emphasis on simplicity and considering the future versatility of iMRS: (1) short-TE (35 ms), PRESS sequences, single voxel, and high field (3 T), which were the same settings as used for preoperative conventional MRS at our institution[16]; (2) placing VOIs at the resection margin with abnormal signals on T2WI or CE-T1WI paying attention only to avoiding contamination from cerebrospinal fluid and hematoma; and (3) making decisions about the residual tumors using only the major absolute metabolite concentrations, Cho and NAA, which were analyzed using the LCModel system. After technical verification, the data obtained using iMRS was of the same high quality as data obtained using preoperative MRS, successfully providing evidence that Cho level and Cho/NAA ratio predicted MIB-1-positive margins with high diagnostic accuracy and that Cho/NAA ratio had a positive correlation with MIB-1 index. Guo et al.[20] attempted to delineate the glioma margin using multivoxel 3-T MRS preoperatively. Consistent with our intraoperative results, they reported a positive relationship between higher Cho/NAA ratio and proliferative potency (MIB-1 ≥1%) at the tumor margin. However, their study provided only information for preoperative surgical planning because they examined abnormal lesions on preoperative MRI scans and not on MRI scans obtained during or after surgery. Our study successfully demonstrated agreement between preoperative MRS and iMRS.

In summary, 3-T iMRS could detect proliferative MIB-1-positive remnants at the resection margin using Cho level and Cho/NAA ratio in the same manner as preoperative MRS. Our results show that single-voxel iMRS could provide information to assist in determining the treatment strategy during glioma surgery. However, this study also had several limitations. First, it was of a preliminary nature and lacked prospective validation of the results. All regions corresponding to VOIs on iMRS were resected based on conventional judgment using abnormal findings on intraoperative MRI because the aim of the study was to verify the

reliability of single-voxel iMRS. There were 5 sites (25%) where no additional excision was required according to retrospective assessment of the histopathological and iMRS results. However, 2 of 3 VOIs in low-grade gliomas were found to be MIB-1-positive, even though low-grade glioma is generally less proliferative than high-grade glioma. Pirzkall et al. reported that regions with a high Cho/NAA ratio could be seen sporadically as "hotspots" in low-grade glioma.[29] Our finding of a positive correlation between Cho/NAA ratio and MIB-1 index indicates that low-grade glioma might have MIB-1-positive spots. In this study, there was no recurrence from regions corresponding to VOIs because all had been resected. However, 5 patients had local recurrence at the resection margins in sites outside of the VOIs. This is a crucial problem with single-voxel iMRS that needs to be resolved in order to improve its utility. For now, it is necessary to understand this limitation and use single-voxel iMRS for glioma surgery. Second, the study was conducted using only conventional MRS parameters, namely, short-TE (35-ms) PRESS sequences. Although there is some controversy regarding these MRS parameters, we have used them to perform preoperative MRS, and previously shown that adequate data differentiating IDH mutation status could be obtained.[16] In this study, we demonstrated that high-quality data could be obtained using iMRS, at least for the same parameters. Third, the number of patients who underwent intraoperative MRI-assisted surgery with iMRS was small, and included those with low- and high-grade gliomas, which had radiologically different behaviors. Fourth, the study was conducted at a single institution. Further prospective studies are thus needed to clarify the methodology of iMRS and the cutoff values for maximal diagnostic accuracy, including which metabolite should be used as an index for differentiating proliferative remnants. Nevertheless, our findings that 3-T iMRS (which has the same parameters as preoperative MRS that take into consideration future versatility) could successfully detect proliferative remnants of glioma are clinically important and demonstrate the potential for practical application of iMRS in glioma

surgery.

Conclusions

This study provides evidence that 3-T iMRS could be performed based on experience using preoperative MRS and intraoperative MRI to detect proliferative remnants at the resection margin using the Cho level and Cho/NAA ratio. Our results show that intraoperative MRI-assisted surgery with iMRS may be useful during glioma surgery.

Acknowledgments: We thank Ms. Takiko Uno for molecular analysis of the isocitrate dehydrogenase mutation status of the patients included in this study.

Funding: This work was supported in part by Grants-in-Aid for Scientific Research from the Japanese Ministry of Education, Culture, Sports, Science and Technology [grant numbers 17K10898 to Eiji Kohmura, 17K10863 to Takashi Sasayama, 17K10864 to Kazuhiro Tanaka, and 15K21146 to Masaaki Kohta]. The sponsor had no role in the study design; in the collection, analysis, or interpretation of data; in the writing of the report; or in the decision to submit the article for publication.

Declarations of interest: None.

References

1. Sanai N, Polley M-Y, McDermott MW, Parsa AT, Berger MS. An extent of resection threshold for newly diagnosed glioblastomas. *J Neurosurg*. 2011;115:3–8. https://doi.org/10.3171/2011.2.JNS10998.

2. Li YM, Suki D, Hess K, Sawaya R. The influence of maximum safe resection of glioblastoma on survival in 1229 patients: Can we do better than gross-total resection? *J Neurosurg*. 2016;124:977–988. https://doi.org/10.3171/2015.5.JNS142087.

3. Beiko J, Suki D, Hess KR, et al. IDH1 mutant malignant astrocytomas are more amenable to surgical resection and have a survival benefit associated with maximal surgical resection. *Neuro Oncol*. 2014;16:81–91. https://doi.org/10.1093/neuonc/not159.

4. Patel T, Bander ED, Venn RA, et al. The role of extent of resection in IDH1 wild-type or mutant low-grade gliomas. *Neurosurgery*. 2018;82:808–814. https://doi.org/10.1093/neuros/nyx265.

5. Pamir MN, Özduman K, Dinçer A, Yildiz E, Peker S, Özek MM. First intraoperative, shared-resource, ultrahigh-field 3-Tesla magnetic resonance imaging system and its application in low-grade glioma resection. *J Neurosurg*. 2010;112:57–69. https://doi.org/10.3171/2009.3.JNS081139.

6. Liang D, Schulder M. The role of intraoperative magnetic resonance imaging in glioma surgery. *Surg Neurol Int*. 2012;3(Suppl 4):S320. https://doi.org/10.4103/2152-7806.103029.

7. Li P, Qian R, Niu C, Fu X. Impact of intraoperative MRI-guided resection on resection and survival in patient with gliomas: a meta-analysis. *Curr Med Res Opin*.

2017;33:621–630. https://doi.org/10.1080/03007995.2016.1275935.

8. Black PM, Alexander E, Martin C, et al. Craniotomy for tumor treatment in an intraoperative magnetic resonance imaging unit. *Neurosurgery*. 1999;45:423–433. https://doi.org/10.1097/00006123-199909000-00001.

9. Reinges MHT, Nguyen H-H, Krings T, Hütter B-O, Rohde V, Gilsbach JM. Course of brain shift during microsurgical resection of supratentorial cerebral lesions: limits of conventional neuronavigation. *Acta Neurochir (Wien)*. 2004;146:369–377. https://doi.org/10.1007/s00701-003-0204-1.

10. Bulik M, Jancalek R, Vanicek J, Skoch A, Mechl M. Potential of MR spectroscopy for assessment of glioma grading. *Clin Neurol Neurosurg*. 2013;115:146–153. https://doi.org/10.1016/J.CLINEURO.2012.11.002.

11. Shimizu H, Kumabe T, Tominaga T, et al. Noninvasive evaluation of malignancy of brain tumors with proton MR spectroscopy. *Am J Neuroradiol*. 1996;17:737–747. http://www.ajnr.org/content/17/4/737.long. Accessed 23 August 2019.

12. Magalhaes A, Godfrey W, Shen Y, Hu J, Smith W. Proton magnetic resonance spectroscopy of brain tumors correlated with pathology1. *Acad Radiol*. 2005;12:51–57. https://doi.org/10.1016/J.ACRA.2004.10.057.

13. McKnight TR, Lamborn KR, Love TD, et al. Correlation of magnetic resonance spectroscopic and growth characteristics within Grades II and III gliomas. *J Neurosurg*.

2007;106:660–666. https://doi.org/10.3171/jns.2007.106.4.660.

14. Devos A, Lukas L, Suykens JAK, et al. Classification of brain tumours using short echo time 1H MR spectra. *J Magn Reson*. 2004;170:164-175. https://doi.org/10.1016/J.JMR.2004.06.010.

15. Choi C, Ganji SK, DeBerardinis RJ, et al. 2-hydroxyglutarate detection by magnetic resonance spectroscopy in IDH-mutated patients with gliomas. *Nat Med*. 2012;18:624–629. https://doi.org/10.1038/nm.2682.

16. Nagashima H, Tanaka K, Sasayama T, et al. Diagnostic value of glutamate with 2-hydroxyglutarate in magnetic resonance spectroscopy for *IDH1* mutant glioma. *Neuro Oncol*. 2016;18:now090. https://doi.org/10.1093/neuonc/now090

17. Pamir MN, Özduman K, Yıldız E, Sav A, Dinçer A. Intraoperative magnetic resonance spectroscopy for identification of residual tumor during low-grade glioma surgery. *J Neurosurg*. 2013;118:1191–1198. https://doi.org/10.3171/2013.1.JNS111561.

18. Roder C, Skardelly M, Ramina KF, et al. Spectroscopy imaging in intraoperative MR suite: tissue characterization and optimization of tumor resection. *Int J Comput Assist Radiol Surg*. 2014;9:551–559. https://doi.org/10.1007/s11548-013-0952-1.

19. Louis DN, Perry A, Reifenberger G, et al. The 2016 World Health Organization Classification of Tumors of the Central Nervous System: a summary. *Acta Neuropathol*. 2016;131:803–820. https://doi.org/10.1007/s00401-016-1545-1.

20. Guo J, Yao C, Chen H, et al. The relationship between Cho/NAA and glioma metabolism: implementation for margin delineation of cerebral gliomas. *Acta Neurochir (Wien)*. 2012;154:1361–1370; discussion 1370. https://doi.org/10.1007/s00701-012-1418-x.

21. Kanda Y. Investigation of the freely available easy-to-use software "EZR" for medical statistics. *Bone Marrow Transplant*. 2013;48:452–458. https://doi.org/10.1038/bmt.2012.244.

22. Bertholdo D, Watcharakorn A, Castillo M. Brain proton magnetic resonance spectroscopy introduction and overview. 2013;23:359–380. https://doi.org/10.1016/j.nic.2012.10.002.

23. Skoch A, Jiru F, Bunke J. Spectroscopic imaging: Basic principles. *Eur J Radiol*. 2008;67:230–239. https://doi.org/10.1016/j.ejrad.2008.03.003.

24. Posse S, Otazo R, Dager SR, Alger J. MR spectroscopic imaging: principles and recent advances. *J Magn Reson Imaging*. 2013;37:1301–1325. https://doi.org/10.1002/jmri.23945.

25. Öz G, Alger JR, Barker PB, et al. Clinical proton MR spectroscopy in central nervous system disorders. *Radiology*. 2014;270:658–679. https://doi.org/10.1148/radiol.13130531.

26. Zhu H, Barker PB. MR spectroscopy and spectroscopic imaging of the brain. *Methods*

Mol Biol. 2010;711:203–226. https://doi.org/10.1007/978-1-61737-992-5_9.

27. Choi C, Ganji S, Hulsey K, et al. A comparative study of short- and long-TE 1H MRS at 3 T for in vivo detection of 2-hydroxyglutarate in brain tumors. *NMR Biomed*. 2013;26:1242–1250. https://doi.org/10.1002/nbm.2943.

28. Provencher SW. Estimation of metabolite concentrations from localized in vivo proton NMR spectra. *Magn Reson Med*. 1993;30:672–679. https://doi.org/10.1002/mrm.1910300604.

29. Pirzkall A, Nelson SJ, McKnight TR, et al. Metabolic imaging of low-grade gliomas with three-dimensional magnetic resonance spectroscopy. *Int J Radiat Oncol Biol Phys*. 2002;53:1254–1264. https://doi.org/10.1016/S0360-3016(02)02869-9.

Figure legends

Fig. 1

(A) Scatter plot demonstrating the correlation between metabolite levels measured using iMRS and MIB-1 index. Respective Pearson's correlation coefficients (r) and significance (p) values are presented. (B) Box plots of metabolite levels measured using iMRS are shown for a positive MIB-1 index and a negative MIB-1 index. Double asterisks (**) indicate a statistically significant difference between the two groups ($P < 0.01$). (C) Receiver-operating characteristic curve showing the accuracy of Cho level (black line) and Cho/NAA ratio (red dot line) for differentiating MIB-1-positive from MIB-1-negative margins (C). Cho, choline; iMRS, intraoperative magnetic resonance spectroscopy; NAA, N-acetyl-L-aspartate

Fig. 2

iMRS in case 4: Axial T2WI shows a hyperintense tumor in the right frontal lobe of a 40-year-old man (A). Intraoperative MRI (sagittal T2WI) shows residual hyperintensity at the ventral and dorsal resection margins and VOIs numbered #4 and #5 are respectively set for iMRS (B). Postoperative MRI (axial T2WI) scan shows gross total resection of the tumor (C). The iMRS waveform has a Cho peak at 3.22 ppm and an NAA peak at 2.02 ppm. iMRS data were quantified using the LCModel system. Absolute metabolite concentrations (mM) of Cho and NAA and Cho/NAA ratio for VOI 4 and VOI 5 are presented (D, E). Photomicrographs of tissue corresponding to VOI 4 and VOI 5 demonstrate immunohistochemically positive (F) and negative (G) staining for MIB-1, respectively. Original magnification ×200. Photomicrograph obtained for diagnosis demonstrates "fried egg" appearance of tumor cells (H). Hematoxylin and eosin staining, original magnification ×200. Histopathological

diagnosis was World Health Organization grade II oligodendroglioma, IDH1-mutant and 1p/19q-codeleted. Cho, choline; IDH, isocitrate dehydrogenase; iMRS, intraoperative magnetic resonance spectroscopy; MRI, magnetic resonance imaging; NAA, N-acetyl-L-aspartate; T2WI, T2-weighted image; VOI, volume of interest

Fig. 3

iMRS in case 7: Axial T2WI showing hyperintense tumor in the right temporal lobe of a 35-year-old man (A). The first intraoperative MRI (coronal T2WI) shows residual hyperintensity at the medial resection margin and VOI 9 is set for iMRS (B). After additional resection, a second intraoperative MRI (coronal T2WI) shows complete resection of the residual tumor (C). Postoperative MRI (axial T2WI) shows gross total resection of the tumor (D). The iMRS waveform has a Cho peak at 3.22 ppm and an NAA peak at 2.02 ppm. iMRS data were quantified using the LCModel system. Absolute metabolite concentrations (mM) of Cho and NAA and the Cho/NAA ratio are presented (E). Photomicrograph of the tissue corresponding to VOI 9 demonstrates immunohistochemically positive staining for MIB-1 (F). Original magnification ×200. Photomicrograph for diagnosis demonstrates microvascular proliferation and high cellularity with polymorphism of tumor cells (G). Hematoxylin and eosin staining, original magnification ×200. Histopathological diagnosis was World Health Organization grade IV glioblastoma, IDH1-mutant. Cho, choline; IDH, isocitrate dehydrogenase; iMRS, intraoperative magnetic resonance spectroscopy; MRI, magnetic resonance imaging; NAA, N-acetyl-L-aspartate; T2WI, T2-weighted image; VOI, volume of interest

Table 1. Patient characteristics

Abbreviations: AA, anaplastic astrocytoma; Cho, choline; DA, diffuse astrocytoma; EOR,

extent of resection; F/U, follow-up; GBM, glioblastoma multiforme; GTR, gross total resection; IDH, isocitrate dehydrogenase; iMRS, intraoperative magnetic resonance spectroscopy; NAA, N-acetyl-L-aspartate; OG, oligodendroglioma; STR, subtotal resection; VOI: volume of interest; WHO, World Health Organization

Table 1 Patient characteristics

iMRS Case No.	Age (years)	Sex	Tumor Location	Pathology	WHO Grade	IDH Status	VOI No.	MIB-1	Resection Margin	NAA	Cho	Cho/NAA ratio	EOR at End of Operation	Recurrence	Recurrence from VOI	F/U (months)
1	33	M	Right insular	DA	II	Mutant	1	1.4	Positive	2.082	2.843	1.37	GTR	No	No	53
2	66	F	Left frontal	GBM	IV	Wild-type	2	8.0	Positive	0.820	0.865	1.05	GTR	Yes: distant	No	12
3	76	M	Left temporal	GBM	IV	Wild-type	3	0	Negative	2.277	0.756	0.33	GTR	No	No	9
4	40	M	Right frontal	OG	II	Mutant	4	1.4	Positive	7.915	2.571	0.32	GTR	No	No	42
							5	0.5	Negative	7.561	1.021	0.14			No	
5	41	M	Right frontal	AA	III	Mutant	6	2.8	Positive	1.007	0.480	0.48	GTR	No	No	41
							7	6.5	Positive	3.148	1.794	0.57			No	
6	62	M	Left temporal	GBM	IV	Wild-type	8	9.5	Positive	4.462	2.736	0.61	STR	Yes: local	No	9
7	35	M	Right temporal	GBM	IV	Mutant	9	13.6	Positive	1.672	3.451	2.06	GTR	Yes: distant	No	33
8	72	M	Left frontal	GBM	IV	Wild-type	10	33.1	Positive	1.665	1.436	0.86	STR	Yes: local	No	11
9	64	M	Right temporal	AA	III	Wild-type	11	5.4	Positive	3.685	1.077	0.29	GTR	Yes: distant	No	16
							12	0.5	Negative	0.192	0.000	0.00			No	
10	45	M	Right frontal	GBM	IV	Wild-type	13	0	Negative	3.089	0.990	0.32	STR	Yes: local	No	12
							14	0	Negative	3.061	0.793	0.26			No	
11	85	M	Right parietal	GBM	IV	Wild-type	15	20.7	Positive	0.726	1.074	1.48	GTR	Yes: distant	No	21
12	82	F	Right frontal	GBM	IV	Wild-type	16	9.2	Positive	3.703	2.021	0.55	GTR	Yes: local	No	15
13	50	F	Right parietal	GBM	IV	Wild-type	17	19.0	Positive	3.651	1.926	0.53	GTR	Yes: distant	No	23
14	37	F	Right insular	AA	III	Wild-type	18	15.5	Positive	5.308	3.667	0.69	STR	Yes: local	No	27
							19	12.9	Positive	3.600	1.395	0.39			No	
15	79	F	Right frontal	GBM	IV	Wild-type	20	0.9	Negative	2.598	1.063	0.41	GTR	Yes: distant	No	9

AA, anaplastic astrocytoma; Cho, choline; DA, diffuse astrocytoma; EOR, extent of resection; F/U, follow-up; GBM, glioblastoma multiforme; GTR, gross total resection; IDH, isocitrate dehydr
iMRS, intraoperative magnetic resonance spectroscopy; NAA, N-acetyl-L-aspartate; OG, oligodendroglioma; STR, subtotal resection; VOI: volume of interest; WHO, World Health Organizatior

ogenase;
า

Fig. 1

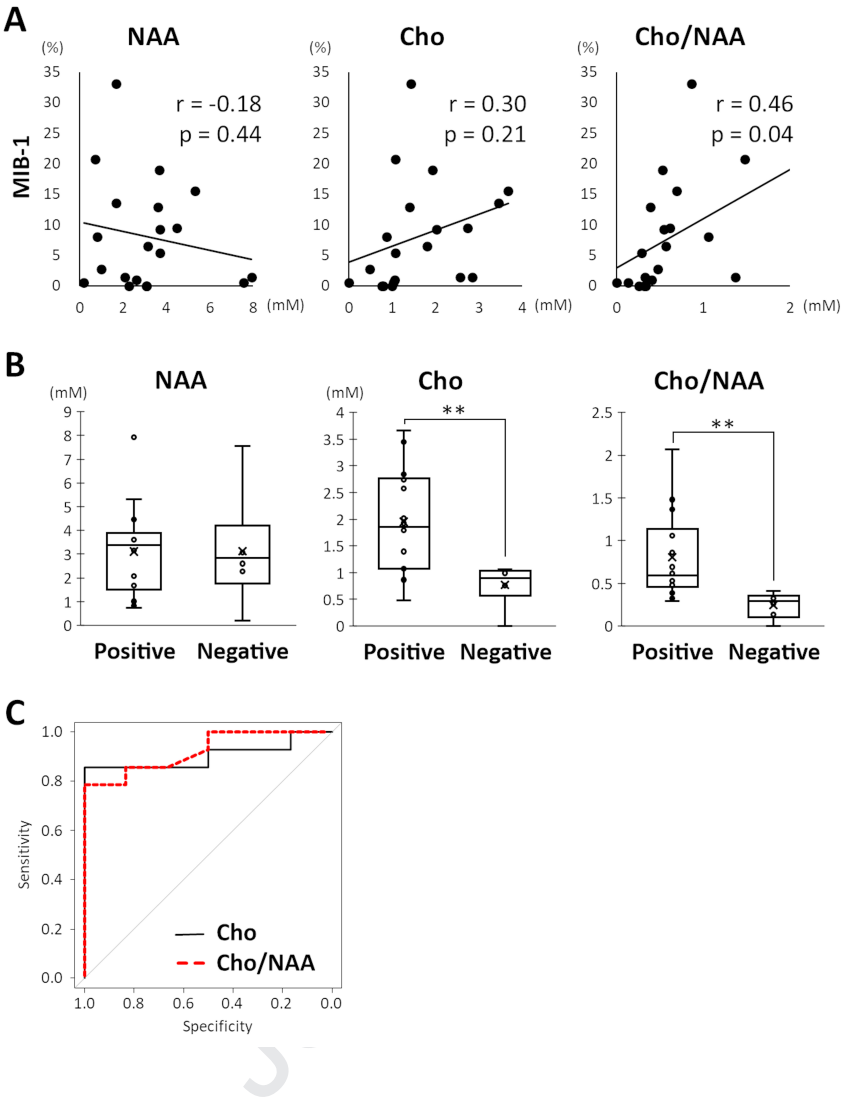
A
NAA
Cho
Cho/NAA
(%)
MIB-1
r = -0.18
p = 0.44
r = 0.30
p = 0.21
r = 0.46
p = 0.04
(mM)
B
NAA
Cho
Cho/NAA
(mM)
**
Positive
Negative
C
Sensitivity
Specificity
Cho
Cho/NAA

Fig. 2

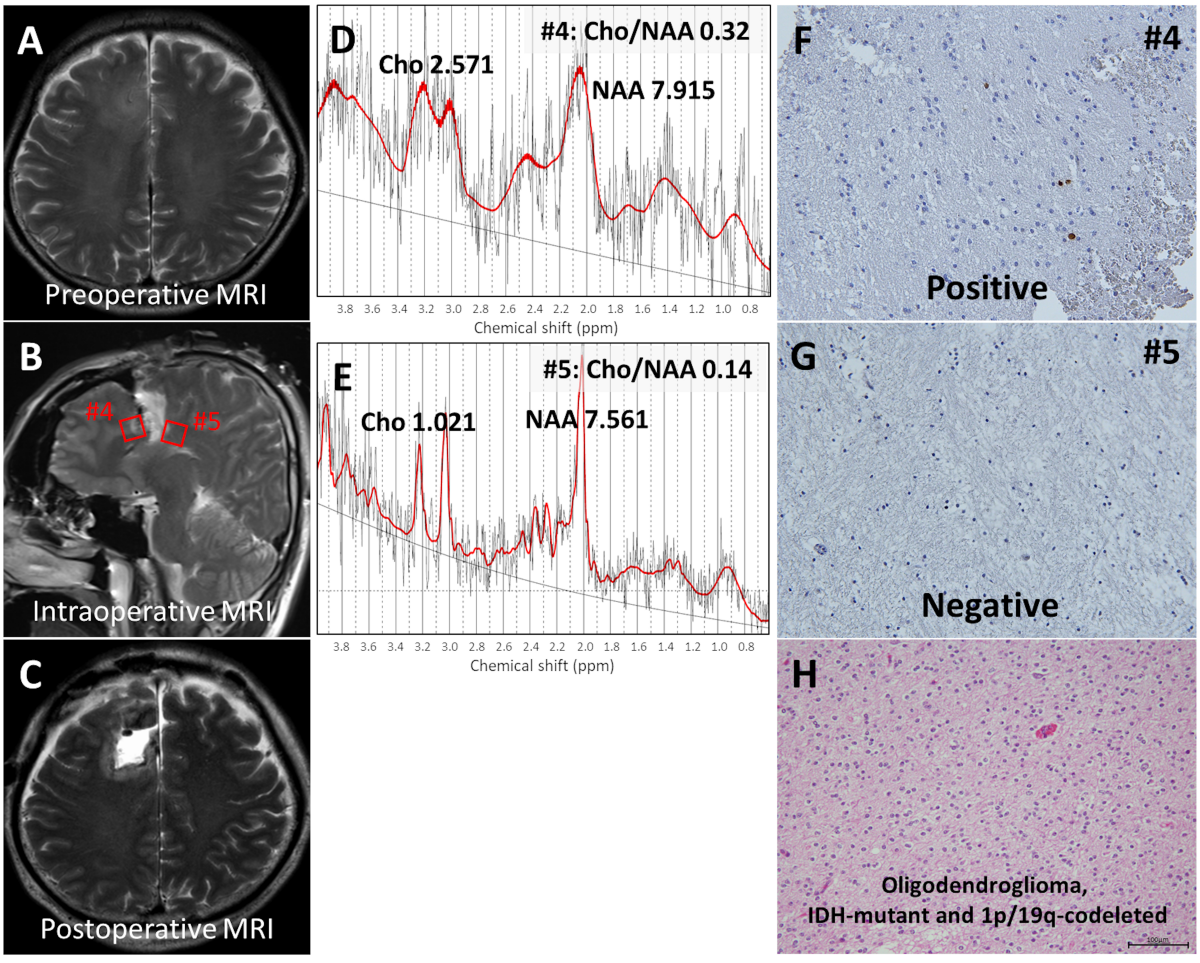
A
Preoperative MRI
B
#4
#5
Intraoperative MRI
C
Postoperative MRI
D
#4: Cho/NAA 0.32
Cho 2.571
NAA 7.915
3.8 3.6 3.4 3.2 3.0 2.8 2.6 2.4 2.2 2.0 1.8 1.6 1.4 1.2 1.0 0.8
Chemical shift (ppm)
E
#5: Cho/NAA 0.14
Cho 1.021
NAA 7.561
3.8 3.6 3.4 3.2 3.0 2.8 2.6 2.4 2.2 2.0 1.8 1.6 1.4 1.2 1.0 0.8
Chemical shift (ppm)
F
#4
Positive
G
#5
Negative
H
Oligodendroglioma,
IDH-mutant and 1p/19q-codeleted

Fig. 3

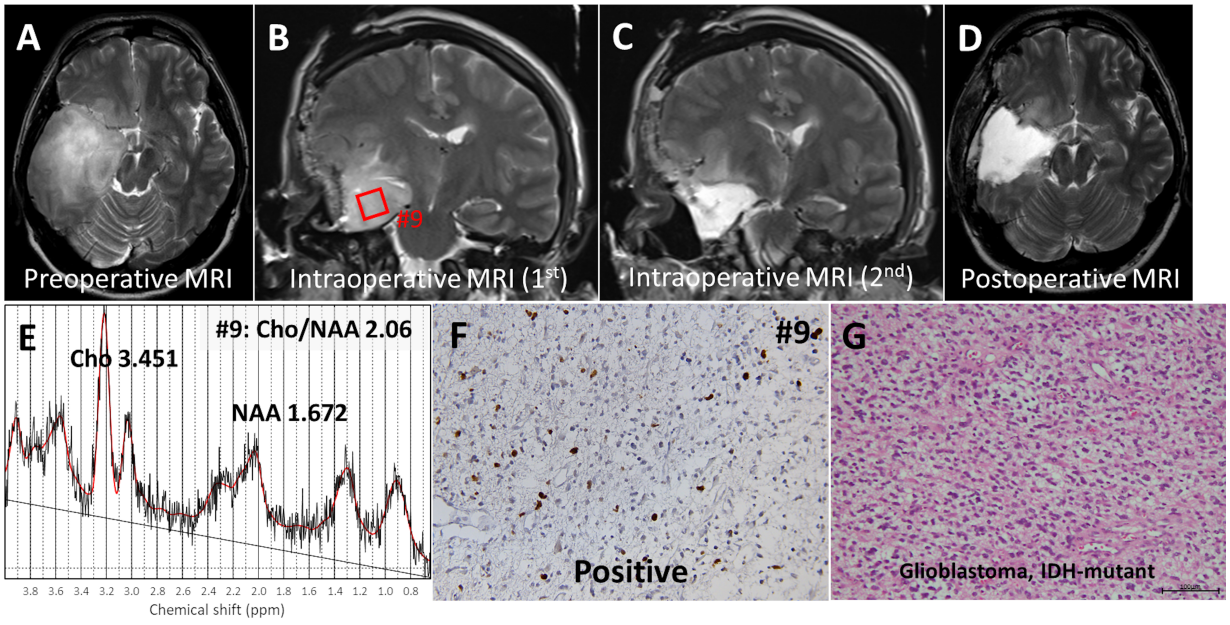

Highlights

- Expertise in preoperative MRS could be in iMRS in glioma surgery
- 3-T iMRS could detect proliferative remnants using the Cho level and Cho/NAA ratio
- 3-T iMRS could assist in determining the treatment strategy during glioma surgery
- Intraoperative MRI-assisted surgery with iMRS may be practicable in glioma surgery

List of Abbreviations

CE, contrast-enhanced

Cho, choline

Cr, creatine

CRLB, Cramér-Rao lower bounds

IDH, isocitrate dehydrogenase

iMRS, intraoperative magnetic resonance spectroscopy

MRI, magnetic resonance imaging

MRS, magnetic resonance spectroscopy

NAA, N-acetyl-L-aspartate

PRESS, point-resolved spectroscopy

T1WI, T1-weighted imaging

T2WI, T2-weighted imaging

VOI, volume of interest

Declaration of interests

☒ The authors declare that they have no known competing financial interests or personal relationships that could have appeared to influence the work reported in this paper.

☐The authors declare the following financial interests/personal relationships which may be considered as potential competing interests: